Single-cell phenotypic plasticity modulates social behaviour in *Dictyostelium discoideum*

Mathieu Forget[a,b], Sandrine adiba[a], Silvia De Monte[a,b]

[a] *Institut de Biologie de l'ENS (IBENS), Département de biologie, Ecole normale supérieure, CNRS, INSERM, Université PSL, 75005 Paris, France*
[b] *Department of Evolutionary Theory, Max Planck Institute for Evolutionary Biology, Plön, Germany*

Abstract:

In *Dictyostelium* chimeric aggregates, strains social behaviour is defined based on their relative representation in the spores, the reproductive cells resulting from development. Some strains, called 'cheaters', that produce more than their fair share of spores are considered a threat to the evolutionary stability of multicellular organization. The selective advantage gained by cheaters is indeed predicted to lead to the progressive loss of collective functions whenever social behaviours are genetically determined and in the absence of mechanisms guaranteeing strong assortment. However, genotypes are not the only determinant of spore bias, and the relative role of genetic and plastic phenotypic differences in strains evolutionary success is unclear.

Here, we control phenotypic heterogeneity by harvesting cells in different growth phases, and study the effects of plastic variation on spore bias in chimeras composed of isogenic or genetically different populations. Our results indicate that variation in cell mechanical properties induced by differences in populations growth phase affects their probability to aggregate, hence their chance to differentiate into spores during multicellular development. The contribution of this non-genetic source of variation to spore bias is non-negligible, and sometimes

*Correspondence:
Email addresses: `forget@bio.ens.psl.eu` (Mathieu Forget), `demonte@bio.ens.psl.eu` (Silvia De Monte)

even overrides genetic differences between co-aggregating strains. These results support the idea that unavoidable variation in the timing of aggregation, a parameter that is not under the control of any single cell or genotype, can compete with selection on genetically determined traits. Our observations suggest that heterogeneity in mechanical properties during aggregation may contribute to limit the spread of 'cheaters', thus to the evolutionary stability of aggregative multicellularity.

Introduction

Dictyostelium discoideum is a model system for studying ecological and evolutionary processes involved in multicellular organization, such as the emergence and stability of cooperative behaviour (Strassmann and Queller, 2011; Forget et al., 2021) cancer (Mathavarajah et al., 2021), as well as the evolution of development (Maeda, 2011; Gruenheit et al., 2018). A constitutive feature of its life cycle – shared by other, independently evolved families of microbes – is that multicellularity ensues from aggregation of cells (Raper, 1940). These cells previously lived and displaced autonomously, so that phenotypically and/or genetically heterogeneous cells can gather in the same multicellular aggregate. Genetic chimeras indeed commonly occur in nature (Fortunato et al., 2003b; Gilbert et al., 2007; Sathe et al., 2013), and are easily produced in the lab upon mixing unrelated clones (Foster et al., 2002). Such chimeras are a precious tool to explore how different genotypes interact in a multicellular context, and to quantify the processes shaping social behaviour of facultatively multicellular species.

In *Dictyostelium*, remarkably, genetic heterogeneity does not disrupt the developmental process: almost all cells that, triggered by starvation, join aggregates differentiate into two terminal fates. One type dies forming the stalk that lifts the other – the spores – above ground and favours their dispersion (Raper, 1940; Smith et al., 2014). When the same amounts of cells of two different strains are mixed, the clone that produces a higher proportion of spores

increases its frequency in the following generation at the expense of the other clone. It is therefore commonly called 'cheater', in analogy to the social strategy of evolutionary games (Hofbauer and Sigmund, 1998; Strassmann et al., 2000). The intensity of cheating behaviour can be quantified by measuring spore bias, that is the difference between the proportion of a clone in the spore pool and its proportion in the initial mix. Spore bias has been proposed as a metric to establish the relation of dominance between couples of strains (Kuzdzal-Fick et al., 2010, 2011; Gilbert et al., 2007; Fortunato et al., 2003a; Buttery et al., 2010) and therefore to identify which genotypes are favoured by natural selection according to their social behaviour. Akin to payoffs in game theory, spore bias measured at different frequencies (the 'spore bias profile') allows to predict the long-term outcome of multiple rounds of aggregation and dispersal, and thus sets the expectations of how evolutionary dynamics would deploy.

Evolutionary predictions and the possibility to compare with theoretical frameworks essentially rely on the association of a given social behaviour (thus spore bias profile) to the genotype of the aggregating types. How a given spore bias gets established is however still unclear, and statistical analyses point to the combination of different factors, including the genetic identity of the focal clone, that of the partner, and additional epistatic effects (Buttery et al., 2009). Even within genetically homogeneous populations, cells have been shown to form spores with different propensity, depending on nutritional history (Leach et al., 1973), cell cycle phase (Zada-Hames and Ashworth, 1978; McDonald and Durston, 1984; Huang et al., 1997; Azhar et al., 2001; Gruenheit et al., 2018), and duration of starvation (Kuzdzal-Fick et al., 2010) among others (see Forget et al. (2021) for a review). Context-dependence can, in particular, give rise to frequency-dependent spore bias profiles with possibly important evolutionary consequences (Madgwick et al., 2018; Rossine et al., 2020).

Here, we aim to experimentally explore: i) the degree of variation in spore profile bias emerging when two phenotypically diverse isogenic populations are mixed; ii) the mechanisms underpinning such bias; iii) whether such plastic variation is large enough to modify biases induced by genetic differences.

Most studies addressing spore bias have so far focused on binary chimeras where the two populations in the mix had discrete phenotypic differences, given for instance by genetic diversity, or by the use of distinct carbon sources. In order to control phenotypic variation more finely, we exploited the observation that phenotypes such as cell volume and cell shape change in the course of demographic growth (Soll et al., 1976; Yuen et al., 1995): cells at the beginning of exponential growth are phenotypically different than those that enter stationary phase. Cell-to-cell differences in growth state at the moment of starvation are expected to occur in natural populations, where the history of cells during vegetative growth may vary greatly even within a single clone, due to different spore germination timing, micro-scale variation in bacteria distribution in the soil, or other sources of environmental fluctuations. The time of harvesting thus acts as a continuous control parameter that allowed us to mix populations – both isogenic and genetically different – in a suite of phenotypic states. This also allowed us to investigate the correlation of spore bias induced by phenotypic heterogeneity and mechanical properties of single cells. Our observations support the previously advanced hypothesis that spore bias is not only shaped by 'social' roles within multicellular aggregates, but also by the way cells self-organize into groups (Dubravcic et al., 2014; Tarnita et al., 2015; Martínez-García and Tarnita, 2016; Rossine et al., 2020). The concept that biases established early in the multicellular life cycle are central to the evolution of social behaviour is further supported by the observation that plastic variation in cell phenotype modulates spore bias also in genetic chimeras. This implies that the selective pressures acting on different genotypes can change significantly on the time scale of the aggregation cycles, hence facilitating the maintenance of strain heterogeneity. On the other hand, the relation between single-cell mechanical properties and biases suggests that the emergence of aggregative multicellularity from unicellular ancestors may have drawn on simple interaction mechanisms, which may have been present in ancestral unicells before the establishment of more sophisticated means of cell-cell communication.

1. Results

We designed an experimental protocol to examine the combined effects of different sources of cell-cell diversity on the social outcome of co-aggregation of two *Dictyostelium* populations, at least one of which is the axenic lab strain AX3 (Loomis, 1971). Plastic variation in cell phenotype at the moment of aggregation were induced by changing the growth phase of vegetative growth where cultures were harvested. Populations progression in the growth cycle is indeed known to induce changes in single-cell properties mediated by the accumulation of secreted factors (Gomer et al., 2011). For instance, cells harvested at low density are round whereas cells harvested at higher density have multiple pseudopodia, hence possibly different mechanical interactions with the environment and other cells (Yuen et al., 1995). Parameters that correlate with spore bias, e.g. cell-cycle phase distribution and nutritional status (Leach et al., 1973; Azhar et al., 2001; Kuzdzal-Fick et al., 2010), are moreover expected to change as a growing population moves from Early Exponential phase (EE), through Mid- and Late Exponential phase (ME, LE, resp.), to Early Stationary phase (ES) and beyond (Soll et al., 1976). A same initial density of cells was grown in standard culture medium for different time intervals, ranging from 24 to 92 hours before harvesting (see Methods, growth curves are reported in Fig. S1). As illustrated schematically in Fig. 1, two populations harvested at different times – thus with presumably different phenotypes – were starved by replacing the growth medium with buffer, then mixed in different proportions at a reference time $t = 0$h. We call chrono-chimeras such binary mixes, whether they belong to the same or different strains. In order to count individual cells belonging to different populations, we used strains transformed with plasmids that bear a fluorescent protein gene (GFP or RFP, see Methods).

Key for assessing spore biases induced in the course of the social cycle is the precise knowledge of the initial fraction f of cells of one, focal type (specified in the following). In order to compensate for inevitable fluctuations induced by dilution, the initial chrono-chimera composition was measured by flow cytometry

(see Methods) just after the cell mix was resuspended in buffer. Starved cells were plated on Phytagel so as to start a standard 'social' cycle, consisting in an aggregation phase (about 8 hours-long) followed by multicellular development, which results in the formation of mature fruiting bodies. Spores were collected after 24h and the fraction of the two differently labelled cells measured with a flow cytometer. The spore bias could be thus estimated as the deviation of the proportion of the focal strain in the spores f_S from that in the initial mix f.

First, we looked at biases in the spores induced by growth phase heterogeneity in isogenic chrono-chimeras. Figure 2 displays the spore bias when populations harvested at different stages of vegetative growth (ME,LE,SE), labeled with GFP, are mixed with a RFP-labeled reference EE population. Insertion of different fluorescent proteins introduced a reproducible bias. Its quantification (see Methods) was used to correct the observed biases by a frequency-dependent term identical for all chrono-chimeras. Our observations indicate that phenotypic differences induced by variations in the start of aggregation relative to the growth phase produce frequency-dependent biases in spore production. Such spore bias profiles resemble in shape and magnitude those observed in genetic chimeras, even though we never observed that spore bias changes sign for intermediate frequencies (Sathe and Nanjundiah, 2018; Madgwick et al., 2018).

Our results reproducibly indicate that ME and LE populations are associated with a positive spore bias when co-aggregating with EE populations (as was previously observed when mixing cultures that had been starved for different periods (Kuzdzal-Fick et al., 2010)). However, such advantage appears to wane for older ES cultures. Different isogenic populations would be therefore alternatively classified as cheaters or cooperators depending on their ecological history at the onset of aggregation, which in natural conditions may not be anticipated by individual cells belonging to any particular strain.

But how does phenotypic heterogeneity at the onset of aggregation influence the outcome of social interactions? Initial phenotypic variation can in principle affect both aggregation and multicellular development, with the latter being considered the step where interactions are properly 'social'. If spore bias mostly

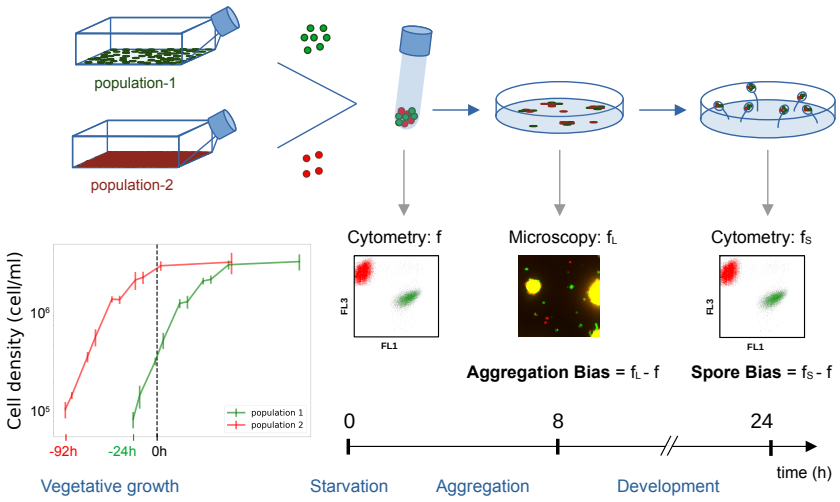

Figure 1: **Schematic representation of the experimental protocol to produce chrono-chimeras.** Differently marked cell populations were harvested at a different phase of their logistic growth (see Fig. S1 for the growth curves of different strains) by starting their culture at different times before the beginning of the experiment. When the culture was started 24 hours before, cells were called Early Exponential (EE), and they were called Mid-Exponential (ME), Late Exponential (LE), or Early Stationary (ES) when they had been cultured for 46, 68 or 92 hours, respectively. As detailed in the Methods, different measures were realized in order to characterize the way biases got established in the course of the multicellular cycle, which was triggered at time $t = 0$ by cell starvation and plating on Petri dishes covered with Phytagel. Before the start of aggregation, the fraction f of cells of one population was measured by flow cytometry. Similarly, the fraction f_S of the same population in the spores was performed after completion of development (24 hours), when spores were collected by washing the Petri dish. Time lapse movies of the aggregation were recorded on an inverted microscope, allowing to count the fraction f_L of cells of each type that remained outside aggregates (the so-called 'loners'). Moreover, measures of single cell properties (discussed later in the text) were realized at $t = 0$ in order to connect initial differences to realized biases.

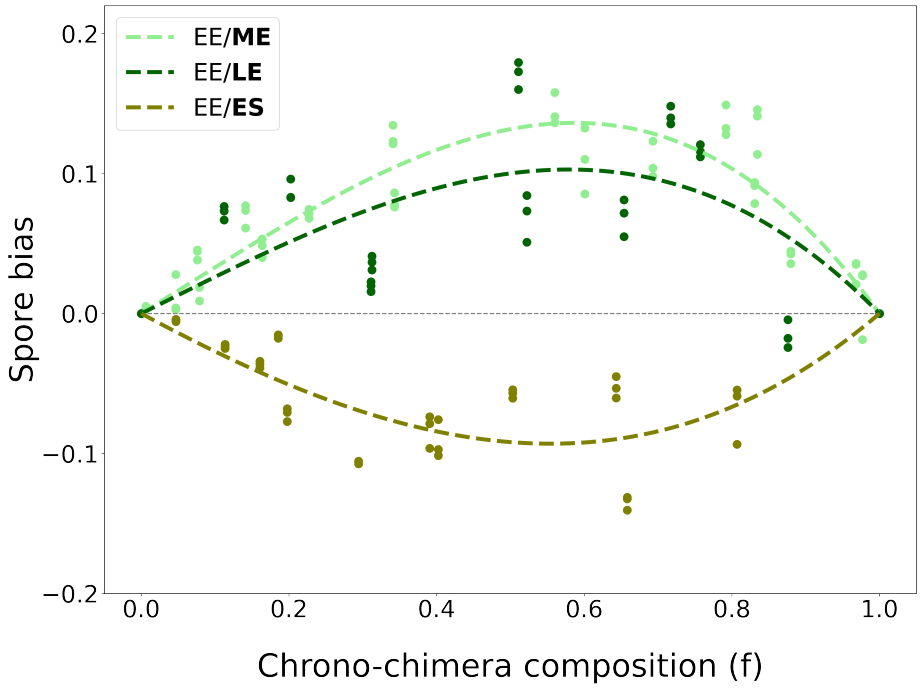

Figure 2: **Frequency-dependent spore bias induced by growth phase heterogeneity.** Corrected (see Methods) spore bias for a focal AX3-GFP population harvested in different growth phases (indicated in bold in the legend), mixed to a reference AX3-RFP EE population. Chrono-chimeras were started mixing different proportions f of the focal strain, so as to assess frequency-dependent effects. Measures of spore bias were realized in three replicates (same initial mix plated on three different plates) and the error bars indicate the standard deviation of the spore measure realized $24h$ later. The observations have been interpolated (dashed lines) with a third degree polynomial constrained with $f = 0$ and $f = 1$.

resulted from processes acting within multicellular aggregates, one should suppose that such interactions were primed by initial phenotypic differences several hours before the aggregation is completed. Such long-lasting phenotypic imprinting may then result in sorting within the slug, as commonly detected when mixing different genotypes (Ennis et al., 2000; McDonald and Durston, 1984; Houle et al., 1989; Escalante et al., 1997). However, we did not detect any noticeable sorting during slug migration (Fig. S4), indicating that social, strategic interactions may not be the main factor determining spore bias differences in

chronochimeras. Alternatively, or additionally, biases may get established early enough, so that initial differences among co-aggregating cells matter, even if these differences are inconsequential at later developmental stages. This hypothesis was proposed in models for the evolution of cells that remain outside aggregates, called 'loners' (Dubravcic et al., 2014; Tarnita et al., 2015; Rossine et al., 2020), where however spore bias was not directly assessed in experiments. We therefore inquired whether the biases observed in isogenic chrono-chimeras could reflect disparate representations of phenotypically different populations in the proportion of aggregated cells. We addressed this question by measuring, at a time when mounds were completely formed (about 8 hours into the social cycle, see Fig. 1), the aggregation bias, *i.e.* the bias in the proportion of cells of the two types among the loners in $f \sim 50\%$ isogenic chrono-chimeras (see Methods). Figure 3 shows that the aggregation bias is negatively correlated to spore bias when chrono-chimeras with different growth differences are taken into account (Pearson correlation coefficient$= -0.58$, $p = 0.01$). It should be noted, however, that the aggregation bias of ES populations varied when the experiment was repeated, possibly reflecting the difficulty of precisely controlling the conditions that cells meet at the entry in stationary phase.

Altogether, our results suggests that a substantial part of the spore bias variation might be attributed to different tendencies of cells to aggregate, depending on their growth phase. In particular, it appears that aggregation happens more efficiently at intermediate times during logistic growth, while cultures that are close to the stationary phase tend to leave more cells behind.

In order to understand how initial phenotypic differences lead to the observed biases in aggregation efficiency, we looked for relevant single-cell parameters that might operate early in the social cycle. Cell adhesion plays a major role in determining how cells get partitioned between aggregated and loner states, and has been explored as one possible mechanism underpinning the evolution of multicellular organization (Garcia et al., 2014, 2015). We characterized the variation during vegetative growth of two types of cellular adhesion: adhesion to a surface and cell-cell adhesion (that can also encompass systems evolved for

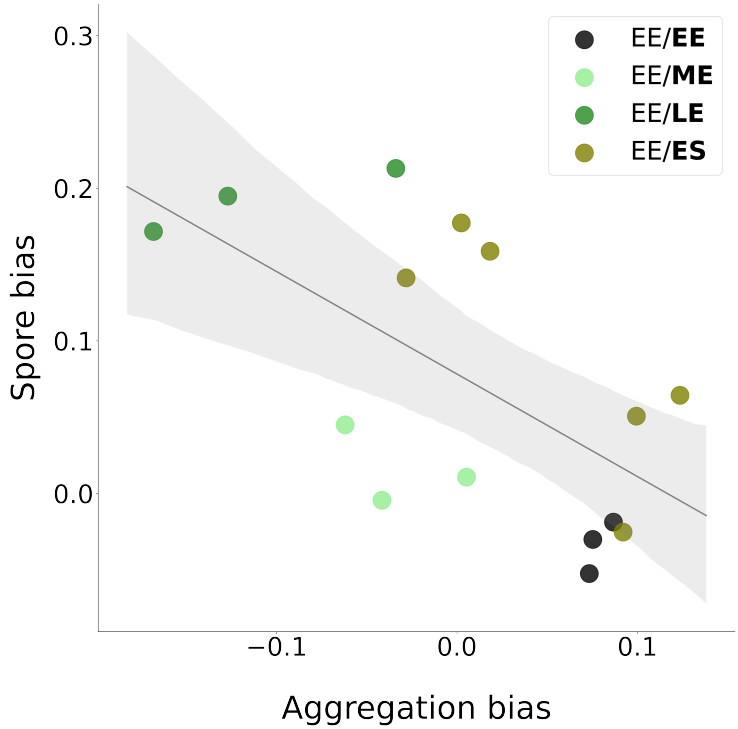

Figure 3: **Spore bias negatively correlates to aggregation bias.** Corrected spore bias (see main text and Methods) as a function of aggregation bias in isogenic chrono-chimeras composed of the strain AX3-GFP with $f \sim 50\%$ of a reference AX3-RFP EE population. The growth phase of the focal population (AX3-GFP) is indicated in bold in the legend.

self-recognition (Hirose et al., 2011)). The former was quantified (see Methods) by measuring the fraction of cells that adhere to a culture vial at low cell density, so that direct interactions among cells should be negligible and our measures pertain to traits of individual cells. Cell-cell adhesion was quantified by measuring the percentage of cells that formed multicellular clusters in shaken cultures (see Methods). Cell adhesion was found to change gradually during demographic growth. Cell-substrate adhesion significantly increases in the course of vegetative growth (Fig. 4 A). Cell-cell adhesion, on the contrary, significantly decreases as a population ages (Fig. 4 B). Studies on the role of differential adhesion in the evolution of social behaviour focused on cell-cell in-

teractions, and predict that less adhesive cells are found more often among the loners (Garcia et al., 2015), which is not what we observe. Another expectation that is not met in chrono-chimeras is that differential cell adhesion would induce segregation of the two co-aggregating populations into aggregates that are mainly composed by one or the other type. We therefore presume that, beyond 'social', cell-cell contacts, cell-substratum adhesion plays a key role in establishing social behaviour, as also supported by recent directed evolution experiments (Adiba et al., 2022).

As amoebae crawl by extending pseudopods (Kessin, 2001), variations in the adhesion to the substratum may alter the probability of aggregation through their effect on cell motility. We tested this hypothesis by measuring individual cell motility in populations harvested in EE, ME, LE, and ES phase.

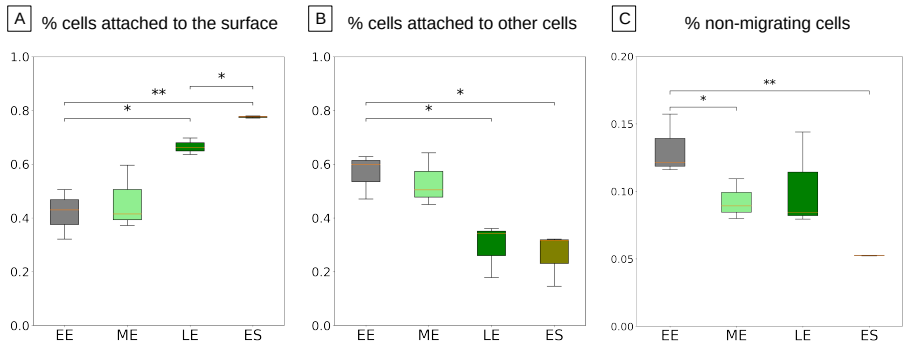

Figure 4: **Variation of cell adhesion and motility properties in the course of vegetative growth of AX3 populations.** Cell-substrate adhesion increases (A), cell-cell adhesion decreases (B) and the proportion of non-migrating cells (see Fig. 5) decreases as a population ages (C). In each assay, three replicates were performed for each condition. *****: Student test p-value < 0.05 ******: Student test p-value < 0.005.

Individual cell motility can be studied by tracking single cells in diluted cultures, so that encounters are rare. We analyzed a large number of cell trajectories ($\sim$ 600 for each condition) in populations harvested at different growth phases and diluted before realizing time-lapse movies (see Methods). Cell position was measured every 30 seconds in the course of 1 hour. The slope

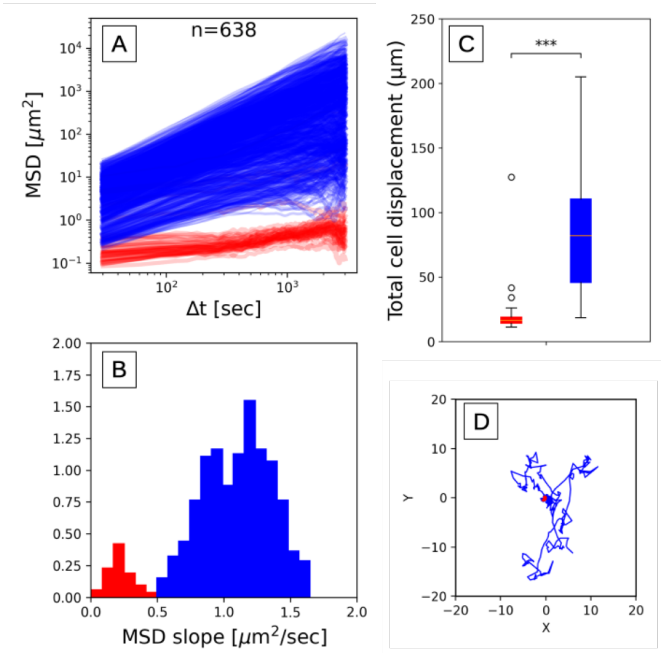

Figure 5: **AX3 populations display a bimodal distribution of cell motility. A:** Individual mean square displacement as a function of time lag (Δt). **B:** Distribution of the initial rate of increase of the MSD (slope of the log MSD vs log Δt, $\Delta t < 150$ secs). Cells were clustered into two motility classes, where such slope was below or above the threshold value 0.5, indicated in all panels in red and blue respectively. **C:** Total displacement of cells from these two classes in the course of 1 hour, showing that the initial slope is a good proxy for how much cells displace (***: Mann–Whitney U test p-value < 0.0005.) **D:** Typical cell trajectories from the two motility classes with their origins brought to a common point illustrating the difference in motility. Results are shown for one LE population (see Figs. S5 and S6 for all replicates and growth phases).

of individual Mean Square Displacement (MSD) as a function of time lag Δt (Fig. 5 A and Fig. S5) reveals the co-existence of two classes of cells with markedly different motility. Figure 5 D shows that part of the cells barely move during the experiment ('non-migrating cells', red), while the others efficiently crawl on the substratum ('migrating-cells', blue). Differences between these classes, quantified for instance by their total displacement, are highly significant (Mann–Whitney U test p-values < 0.0005 , Fig. 5 C and Fig. S6). A bimodal

distribution of cell motility is consistent with a previous analysis of a small number of *Dictyostelium* AX2-cells just before starvation ($\sim$ 40 cells) (Goury-Sistla et al., 2012)). Our observations reveal that demographic growth influences population partitioning in the two motility classes more than cell speed within each of the classes – no significant variation in total displacement of migrating cells was observed between populations harvested in different growth phases (mixed effects model ANOVA, p-value=0.4691, Fig. S6). Figure 4 C shows that the percentage of low-motility cells decreases as the cell culture ages. By comparing these results to variations in adhesion, we can speculate that cells belonging to the low motility class also adhere less to the surface and are more likely to end up as loners.

A progressive decrease in the fraction of non-migrating cells, which are more likely to remain outside aggregates, could thus explain why ME and LE cultures tend to have a positive bias relative to EE/EE chrono-chimeras. However, in order to explain the decrease of the bias observed in EE/ES chrono-chimeras, other yet uncharacterized mechanisms should be identified.

We showed that spore biases can vary as a consequence of single-cell variability appearing during vegetative growth. Although we expect that the temporal variation in cellular features is general, it might however be inconsequential when populations that are mixed have large, intrinsic phenotypic differences, for instance those induced by distinct genetic identities. We thus considered chrono-chimeras obtained by mixing strains that had from the start large biases in spore production. We compared spore bias for different compositions of the chimera, in three conditions: when the two strains were both harvested in the ME phase (see Fig. S1 for the growth curves of different strains), when the focal strain was in EE and the other in LE, and vice-versa. We expected that the latter two conditions would induce a bias in opposite directions relative to the 'baseline' bias observed when the two strains were grown for the same, intermediate, duration before harvesting.

In line with the hypothesis that adhesion plays a key role in determining the efficiency of aggregation, we started examining chimeras composed of strains

with highly divergent cell-substratum adhesion. The AX3-Bottom strain was evolved from the ancestral AX3 strain by imposing selection for increased adherence to the bottom of a culture vial, and has a strong spore bias relative to the ancestor (Adiba et al., 2022). Differences between AX3 and AX3-Bottom are not known at the genotypic level, but these strains are expected to diverge chiefly for the phenotype that was under selection (single cell adhesion to the substrate). Compared to the 'baseline' bias observed when the strains are harvested at the same time, the bias increases or decreases depending on whether the focal strain is harvested later or earlier (Fig. S7 A). Consistent results are obtained when the more advanced population is harvested in ME phase rather than in LE phase (Fig. S7 B). These observations indicate that spore bias is concomitantly affected by plastic variation and phenotypic differences resulting from selection on single-cell adhesion. Nonetheless, even though growth differences modify the bias, they are not sufficient to alter the qualitative classification of social behaviour, and the ancestor strain keeps being classified as a cheater.

A similar growth phase-dependent variation in the bias was obtained in chrono-chimeras where the reference strain AX3 was mixed with another strain derived from an AX3 ancestor, the well-known cheater strain chtA . chtA displays the most extreme and disruptive form of selfish behaviour, obligate cheating: it is unable to form spores when developing clonally, but induces its ancestor to differentiate into stalk (Ennis et al., 2000). Consistent with this classification, we found that the AX3 strain had a negative bias when harvested at the same time as chtA (Fig. 6 A). Such bias tends to increase when AX3 is harvested in EE phase and chtA in LE phase, but is reduced to almost zero for the reversed phase relation (when AX3 is in high proportion in the chrono-chimera), confirming again that populations in different growth states can produce variable contributions to the spore pool, thus affecting the pace of evolution of social behaviour even when the social phenotypes are very different.

AX3-Bottom and AX3-chtA were obtained by artificial selection (directional selection of single-cell adhesion and mutagenesis followed by screening for strong

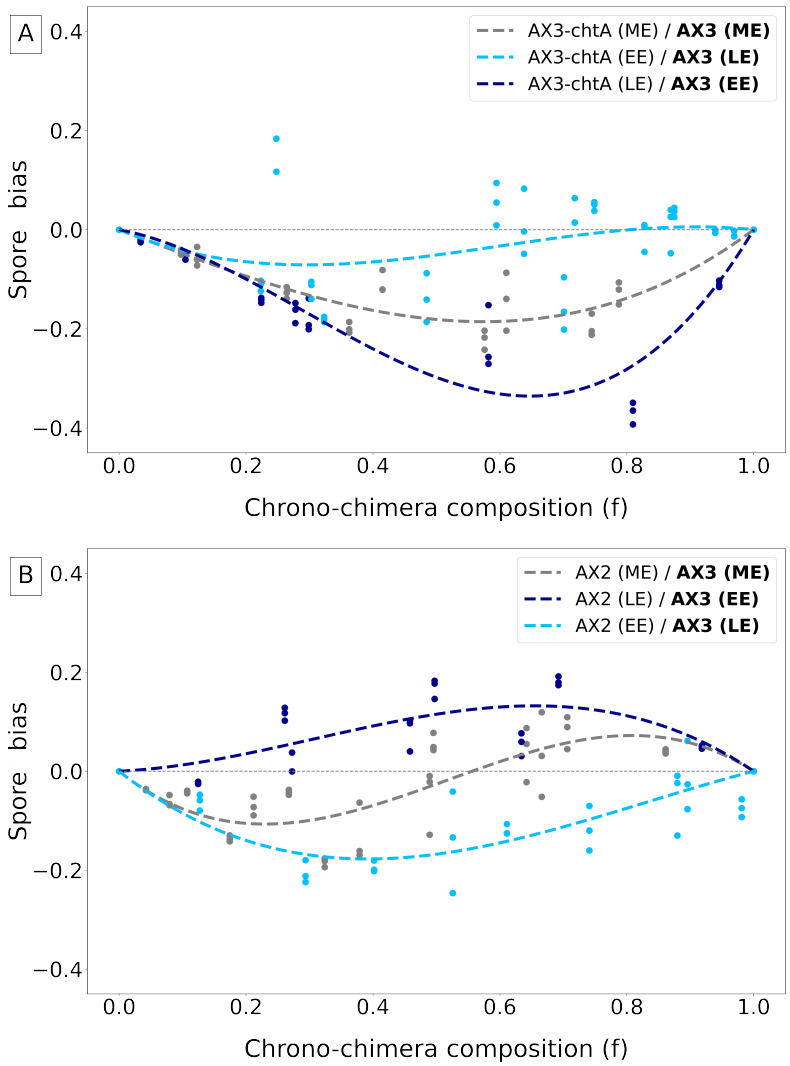

Figure 6: **Social behaviour in chimeras depends on populations growth phase at the onset of aggregation.** Spore bias measured in two different genetic chimeras, using a population of AX3-RFP cells as the focal population. **A:** chrono-chimeras composed of AX3-RFP and chtA cells. **B:** chrono-chimeras composed of AX3-RFP and AX2 cells. Three different cases are considered: strains are grown in co-culture and harvested in ME phase, the focal population is harvested in EE phase and the other in LE phase (dark blue line), or vice-versa (light blue line).

spore biases, respectively). Correspondingly, they manifest extreme social behaviours. However, in natural conditions co-aggregating strains, likely evolved under selective pressures that were both weaker and acting on many traits simultaneously, may not be as phenotypically divergent. We examined chrono-chimeras for another pairwise combination of strains, where AX3 was mixed with the axenic strain AX2. Both these strains derive from the same natural isolate (NC-4), but have genome-wide differences: AX3 carries a large duplication, corresponding to 608 genes, compared to AX2 (Sucgang et al., 2011). Despite such large genomic differences, AX2 is not known to display a marked social behaviour with respect to AX3. Indeed, we found that, in the absence of growth phase heterogeneity, AX3 cells co-aggregating with AX2 cells are under-represented in the spores when in low proportion in the chimera, whereas they are associated to a positive spore bias when prevalent (Fig. 6 B). In this chrono-chimera, depending on the growth phase of the two populations, the focal strain AX3 shifts from behaving like a cheater (when it is harvested in EE while AX2 is in LE) to behaving as a cooperator (in the opposite case). In genetic chronochimeras, however, there does not seem to be a constant relation between a specific growth phase difference and social behaviour: in AX3/AX2 chimeras later cultures tend to be negatively biased, and vice-versa in AX3/AX3-chtA chimeras, despite apparently very similar demographic growth (Fig. S1).

Taken together, results on chrono-chimeras involving different strains indicate that the effects of growth phase-induced phenotypic differences at the time of aggregation on social behaviour combine with those due to genetic diversity. The contribution of these two sources of variation to spore bias is not additive. Instead, the effect of population growth phase differences depends on the chimeras genetic background (Fig. S8). In some cases, growth phase-induced phenotypic differences can reverse the classification of a strain from cheater to cooperator. As the highly controlled timing of aggregation that is imposed in lab experiments is unlikely to reflect natural conditions, it is therefore plausible that commonly used methods for classifying social behaviour may bear little information on the expected evolutionary outcomes of strain interactions in the

wild.

2. Discussion

Social interactions of cells within multicellular structures are essential to ensure their coherent collective functioning. Division of labour, whereby different cells take up different collective tasks, is essential for many such functions, but is often associated to differences in reproductive success among distinct cell phenotypes. Such differences are particularly threatening for multicellular function when they are transmitted across generations of the collective association. In aggregative microbes like *Dictyostelium discoideum*, where multicellular groups are formed by gathering cells that can be genetically heterogeneous, cell types that are overrepresented in the spore pool have the potential to get progressively enriched in the population over successive aggregation cycles. Crucial for this to occur is however a heritable relation between cell genotype and its reproductive success. This is realized when the outcome of social interactions is by and large genetically determined, as assumed by the theory of sociobiology (Strassmann and Queller, 2011; Forget et al., 2021).

Several recent studies have started to question the relevance of this assumption for *Dictyostelium* and revealed complex relationships between properties of single cells and their reproductive success. Madgwick et al. (Madgwick et al., 2018) proposed that the variation of spore bias with the composition of chimeras between two natural strains is best explained if the probability of becoming a spore is adjusted in response to the multicellular context. In this perspective, cheating would result from 'strategic' choices of each cell, influenced for instance by the diffusion of morphogens during multicellular development (Parkinson et al., 2011). Therefore, a same cellular genotype could give rise to multiple possible biases depending on how many and what kind of cells happen to surround a focal cell. Our results confirm that spore biases depend on the nature of the social partner also in isogenic chrono-chimeras: a population harvested in early exponential phase can be associated to a positive or a negative spore

bias, depending on the growth phase of the co-aggregating population, and the intensity of the bias depends on the composition of the mix (Fig. 2). Our observations however suggest that biases are, at least in part, established ahead of multicellular development, during aggregation. Aggregation biases can result from pre-existing differences in single-cell phenotypic properties, and do not necessarily require 'negotiations' involving a multitude of cells.

Similar conclusions on the early establishment of biases during cell aggregation was drawn by researchers addressing the evolutionary role of loner cells (Dubravcic et al., 2014; Tarnita et al., 2015; Rossine et al., 2020). While in early models the hypothesis was formulated that the probability of aggregation (hence the ensuing spore bias) was determined by the strain genotype, recent progress confirmed that the situation is more complex, and context-dependence widespread (Dubravcic et al., 2014; Rossine et al., 2020). Indeed, a same strain can produce a different number of loners depending on its own and the other strain's cell density. A mathematical model was used to show that differences in the sensitivity to an aggregation signal induce frequency-dependent aggregation biases whose variability can be leveraged for maintaining - over multiple social cycles - a coexistence of different genotypes. The correlation we observed between aggregation and spore bias supports the notion that biases are broadly set by the end of the aggregation phase.

Based on the observed correlation between aggregation bias and single-cell mechanical properties, we propose that signals - or other social interactions involving a large number of cells - aren't strictly necessary to account for differences in aggregation propensity (at least as long as the culture is sufficiently far from stationary phase). Instead, differences in cell adhesion or motility, thus properties that can evolve independently of their social context, may be sufficient to influence cells assembly into groups, as advanced by some theoretical studies (Garcia et al., 2014, 2015; Arias Del Angel et al., 2020; Forget et al., 2022). If a fraction of cells does not attach to the surface and is unable to actively migrate towards the aggregation centers, the population where this is largest will automatically be underrepresented in the spores – unless develop-

ment reverses the bias.

We do not know by what means differences in populations growth phase produce variations in the proportion of non-migrating cells. It is nonetheless plausible that they result from changes in the distribution of cells within the cell cycle. When a population ages, indeed, the fraction of actively dividing cells (in the S/M phase of the cell cycle) decreases (Soll et al., 1976; Zada-Hames and Ashworth, 1978). *Dictyostelium* cells entering cytokinesis tend to round up and to be less adhesive to the substratum (Nagasaki et al., 2002; Plak et al., 2014). As a consequence, they may contribute disproportionately to the pool of non-migrating cells that end up not joining any aggregate. The hypothesis that isogenic cultures harvested at later times produce a higher proportion of aggregating cells with respect to early exponential phase is not only consistent with our observations of progressive modifications of single-cell adhesion and motility. It also provides a mechanistic explanation to the previously reported negative correlation between the fraction of cells in S/M phase in a population and its probability of forming spores (Azhar et al., 2001; Huang et al., 1997; Gruenheit et al., 2018).

Growth phase differences are just one possible non-genetic source of cell phenotype variation that affects representation in the pool of spores. Plastic heterogeneity could be caused by both environmental and physiological variation (Leach et al., 1973; Kuzdzal-Fick et al., 2010; Kubohara et al., 2007; Hiraoka et al., 2020). How it gets transmitted across the aggregation phase and through multicellular development is however still unclear. Indeed, *Dictyostelium* social cycle involves important changes in gene expression (Coates and Harwood, 2001; González-Velasco et al., 2019), so that phenotypic variation induced during vegetative growth should in principle fade shortly after the beginning of the social cycle. On the other hand, non-aggregated cells are irreversibly excluded from multicellular development. Whether differences in aggregation efficiency can explain biases in isogenic populations derived from other sources of plastic variation and superpose as well to genetic effects will require further exploration.

Single-cell phenotypic heterogeneity can influence aggregation probability ir-

respective of its genetic or non-genetic origin. However, its underpinning and the way it gets transmitted along the social cycle are important to understand the evolutionary consequences of social behaviour. In particular, the prediction that 'cheaters' have a long-term advantage could be upended if short-term measures of reproductive success do not carry over to successive generations, so that relevant variation is effectively neutral (Arias Del Angel et al., 2020; Nanjundiah, 2019). Our results point to a role of unpredictable variation that may be much larger than previously considered when associating a genotype to a social behaviour. Indeed, the social cycle of *Dictyostelium* can involve not only cells with a distinct genetic background, but also cells that are in different states of growth. As a consequence, single-cell properties at the moment of aggregation and the derived biases are not only shaped by the genetic identity of a strain, but also by factors that are not under direct genetic control. Such factors have more to do with the ecological history of individual cells (e.g. how much food they collected, when exactly they starve) and its consequences on cell mechanics than with a genetically-determined behaviour in a multicellular, social context. We can thus speculate that spore bias variability may have similar underpinnings in chimeras composed of both isogenic cells and distinct strains. If such explanation holds true also in natural populations, it may contribute to understanding how aggregative multicellular life-cycles persist on evolutionary times despite unavoidable genetic conflicts.

Material and Methods

Strains and media

Dictyostelium discoideum strains used in this study are AX3 (Dictybase ID: DBS0235545), AX3-chtA (Dictybase ID: DBS0236369), AX2 (donation by Clément Nizak), and the AX3-Bottom line (Adiba et al., 2022). AX3-GFP and AX3-RFP cell lines were obtained by transforming AX3 cells with plasmids pTX-RFP (Dictybase ID: 112) or pTX-GFP (Dictybase ID: 11) (Dubravcic et al., 2014). Both plasmids carry a gene for antibiotic resistance (Gentamicin 418, Sigma-Aldrich: G418). Vegetative growth was started from frozen aliquots thawed every week to prevent the accumulation of undesired mutations due to prolonged culturing. Cells were grown in autoclaved HL5 medium (per L, 35.5 g HL5 from *formedium*, pH=6.7) at 22°C with a concentration of 300 µg mL^{-1} Streptomycin. Additional 20 µg mL^{-1} G418 were supplemented when growing transformed strains. Pre-cultures were prepared by thawing frozen aliquots and growing in 25 cm^2 TC treated flasks (*CytoOne* CC7682-4825) with 10 mL culture medium for 30 hours, which allows the population to restart and enter the exponential growth phase. Cells were grown in static cultures to limit the risk of impaired cytokinesis as observed in shaken suspension. SorC buffer was prepared with 0.0555 g $CaCl_2$; 0.55 g Na_2HPO_4 $7H_2O$; 2 g KH_2PO_4 per Liter.

Strains growth kinetics

Growth kinetics of AX3-GFP, AX3-RFP, AX3-Bottom, AX3-chtA and AX2 were characterized to estimate the timing of their growth cycle under the experimental conditions (Fig. S1). Pre-cultures were diluted to 10^5 cells/ml and re-suspended in fresh medium. At each time point, cell density was scored using an hemocytometer. Three replicate cultures were scored in parallel for each strain.

Starvation protocol

In order to trigger *Dictyostelium* social cycle, cell populations were starved by washing out the nutrient medium via three successive centrifugations with buffer at 4°C (2000 rpm for 7 min). Cells were kept on ice between successive rounds of centrifugation. After the last centrifugation, the pellet was resuspended in buffer and the cell density adjusted to 2.10^7 cells mL^{-1}.

Chrono-chimeras preparation

Chrono-chimeras are composed of a mix of starved cells from two populations harvested at different times during vegetative growth, *i.e* in different growth phases at the time the experiment was begun ($t = 0$, Fig. 1). Each population was started from a pre-culture diluted in fresh medium to 10^5 cells mL^{-1}. In order for them to attain different growth phases at the beginning of the experiment (established based on the growth kinetics displayed in Fig. S1), cultures were started a fixed number of hours before the beginning of the experiment: 24h hours for early-exponential phase (EE); 46 hours for mid-exponential phase (ME); 68 hours for late-exponential phase (LE) and 92 hours for early-stationary phase (ES). Transformed cells used in isogenic chronochimeras had indistinguishable growth curves (Fig. S1 A), so that there was a precise correspondence between the phase of growth and the density of cells at the moment of harvesting.

At $t = 0$h (Fig. 1), the two cultures were starved as described in the previous section. Starved cells from the two populations were then mixed so as to attain a target proportion. Deviations from the target proportion sometimes occurred due to fluctuations in dilution. The actual mix composition f was thus quantified by measuring the proportion of labelled cells by flow cytometry (Cube8 cytometer, using Forward Scatter (FSC), Side Scatter (SSC), fluorescence channels : FL1 (GFP) and FL3 (RFP)). The accuracy of this measurement was first validated by comparison with manual countings with a hemocytometer. A volume of 40 µL of the mix (corresponding to 8.10^5 cells) was then plated on 6 cm

Petri dishes filled with 2 mL of 2% Phytagel (Sigma-Aldrich), following Dubravcic *et al* (Dubravcic et al., 2014). Cells were then incubated for 24 hours at 22°C. For each mix, three technical replicates were performed by plating three 40 µL droplets of cell suspension on 3 different Petri dishes.

Quantification of spore bias in chrono-chimeras

24h after plating, spores were harvested by washing the three Petri dishes corresponding to the three technical replicates in 500 µL SorC buffer. Spores suspensions were incubated for 5 minutes with 0.5% Triton X-100 and then centrifugated for 7 min at 2000 rpm to remove stalk cells or unaggregated cells that would have survived the 24h-starvation-period. Finally, the pellet was re-suspended in 800µL SorC buffer and the proportion of GFP and/or RFP-spores was scored using a cytometer. Spore bias of the focal population was quantified as the deviation between its proportion in the spores f_S and its proportion f in the initial mix.

To quantify the effect of growth phase heterogeneity on spore bias, we quantified spore bias in chrono-chimeras composed of cells harvested in EE, ME, LE and ES phases of vegetative growth. Starting from the same batch of frozen aliquots, we tested a range (between 7 and 15 for each binary combination) of proportions f to assess frequency-dependent effects on spore bias. In principle, transformed strains were expected to produce no bias upon co-aggregation if the inserted fluorescent markers were strictly equivalent. However, we realized that chimeras composed of AX3-RFP and AX3-GFP cells grown in co-culture and both harvested in EE phase yielded a reproducible and significant bias (Fig. S2). The same bias was observed after having repeated the transformation protocol. In order to compensate for such labelling effect on spore bias, we substracted from our measures of the spore bias the bias predicted based on co-culture of differently labeled populations. Such intrinsic bias was computed for every frequency by interpolating with a third degree polynomial constrained with $f = 0$ and $f = 1$ (Fig. S2). In order to validate the use of this correction, we con-

firmed that spore biases are reversed when the fluorescent labels are swapped (Fig. S3).

Quantification of aggregation bias in chrono-chimeras

Aggregation bias was estimated in chrono-chimeras composed of a comparable number of cells from the two populations (*i.e* $f \sim 0.5$). Chrono-chimeras were prepared as previously described and plated on a Petri dish that was scanned and imaged at regular time intervals (5 min). Images were taken with an automated inverted microscope Zeiss Axio Observer Z1 with a Camera Orca Flash 4.0 LT Hamamatsu, using a 10X objective, which yielded phase contrast and fluorescence images. Cell aggregation was considered complete when the last streams disappear. At that time, the number of unaggregated cells from the two populations was scored. Images corresponding to different areas of the Petri dish were first analysed using ImageJ software (Schindelin et al., 2012): aggregates were manually contoured and discarded and the "Find edges" ImageJ function was applied to highlight the contour of individual unaggregated cells. f_L, the fraction of loners produced by the focal population, was then estimated on several images as the number of unaggregated cells from this population divided by the total number of unaggregated cells. Based on this observable we were able to quantify the bias in the fraction of unaggregated cells as the deviation between the proportion of cells from the focal population found in the pool of unaggregated cells (f_L) and f.
The chrono-chimeras for which we measured the aggregation bias in parallel of the spore bias (Fig. 3) were started from a stock of frozen aliquots with higher initial cell density than that used to measure spore bias for a range of f values (Fig. 2). If spore bias variation is overall consistent, the EE/ES chimeras showed a more variable and mostly positive spore bias.

Motility assay

Cells were first starved as previously described. After the last centrifugation, the pellet was re-suspended in 3 ml of buffer with a density of 10^4 cells

mL^{-1}. This cell density was sufficiently low for cells not to touch with one another during the assay. The cell suspension was then poured in an empty 6 cm Petri dish. After 30 min –the time for the cells to attach to the bottom of the dish– cells trajectories were tracked for 1h (one image per 30 seconds) under an inverted microscope equipped with a moving stage and a 5X objective (alike to the measure of 'aggregation bias'). A large area of the Petri dish was scanned to analyze around 600 cells trajectories per sample. Cell trajectories were then automatically extracted from the time lapse movies using the Python package *Trackpy* (Allan et al., 2018). Three biological replicates were imaged for populations harvested in EE , ME , LE and ES phase. Another script was used to analyse trajectories. Mean square displacement (MSD) was computed as a function of time lag for every single cell. The slope of the log(MSD) vs log(time lag) curve at low Δt values ($\Delta t < 150$ seconds) was used as a criterion to distinguish slowly moving (slope $<$ threshold) from fast-moving cells (otherwise). The threshold value was set to 0.5 in order to separate the two modes of the slope distribution (Fig. S5), and the proportion of cells belonging to each class was scored. Individual cell total displacement was quantified as the sum of cells displacement between two successive frames along the trajectory.

Cell-substratum adhesion assay

Cell-substratum adhesion was quantified based on cells' ability to attach to the bottom of a TC treated culture flask *(CytoOne, CC7682-4325)* as in Adiba et al. (2022). Cells were first starved as previously described. After the last centrifugation, the pellet was re-suspended in 10 ml buffer and cell density was adjusted to $2,5.10^5$ cells mL^{-1}. The cell suspension was then incubated in a 25 cm^2 flask (*CytoOne* CC7682-4825) for 30 minutes at 22 °C, the time for cells to attach to the bottom of the flask. Each culture flask was gently shaken to re-suspend cells that are not attached to the bottom of the flask. The supernatant (containing unattached cells) was transferred into a 15 *ml* tube. Cell density in the supernatant was measured using a hemocytometer. The fraction of adhe-

sive cells was obtained by dividing the density of cells in the supernatant by the total cell density inoculated in the flask and used as a proxy for cell-substrate adhesion level. This assay was performed on three biological replicates for populations harvested in EE , ME , LE and ES phase.

Cell-cell adhesion assay

Cell-cell adhesion was quantified by a modified method of Gerrish (Gerisch, 1968). Cells were first starved as previously described. After the last centrifugation, the pellet was re-suspended in 0.5 ml buffer at a density of 10^6 cells mL^{-1}. The cell suspension was rotated at 150 rpm and 22°C for 1 hour, allowing cells to form multicellular clumps. The number of unaggregated cells (singlets and doublets) was determined using a hemocytometer. The percentage of cells that had been recruited into aggregates was calculated as the total cell density minus the density of unaggregated cells, divided by the total cell density. This quantity was used as a proxy for cell-cell adhesion level. The assay was performed on three biological replicates for populations harvested in EE , ME , LE and ES phase.

Statistical analysis

Significance of pairwise comparisons was established based on two-sample Student t test or Mann–Whitney U test using the python module *Scipy* (Virtanen et al., 2020). Significance of the effect of populations growth phase on cells' total displacement was tested with a linear mixed effects model using replicates as random effects ('nlme' library, R). The significance level was set equal to 5%.

Supplementary Information

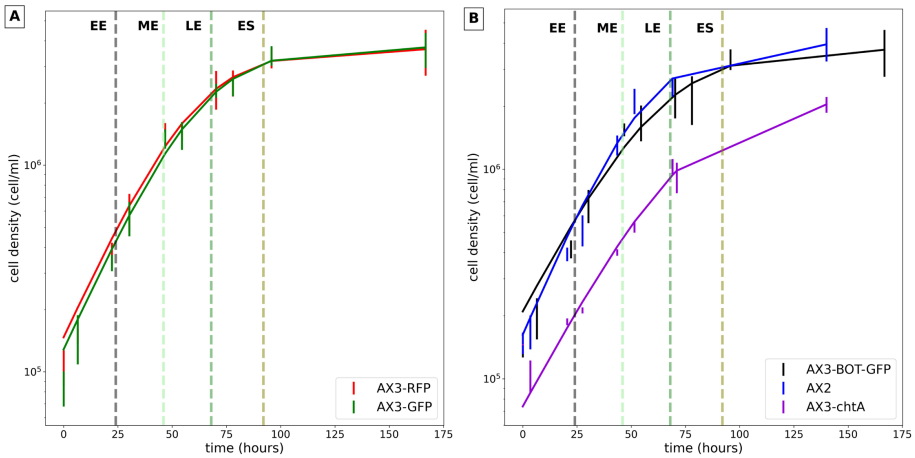

Figure S1: **Growth kinetics of the different strains used in the experiments.** Cell density of cell cultures grown in 25 cm^2 culture flasks with 10 ml HL5 medium were assessed using an hemocytometer. Before the beginning of the experiment, pre-cultures were prepared from frozen aliquots as described in the Methods. (A) Isogenic, transformed populations AX3-RFP, AX3-GFP. (B) Strains that were derived from an AX3 ancestor (AX3-Bottom-GFP and AX3-chtA), and the strain AX2 that has a more distantly related ancestor. All strains had similar growth kinetics, but ChtA's initial density was slightly lower due to fluctuations at the moment of dilution.

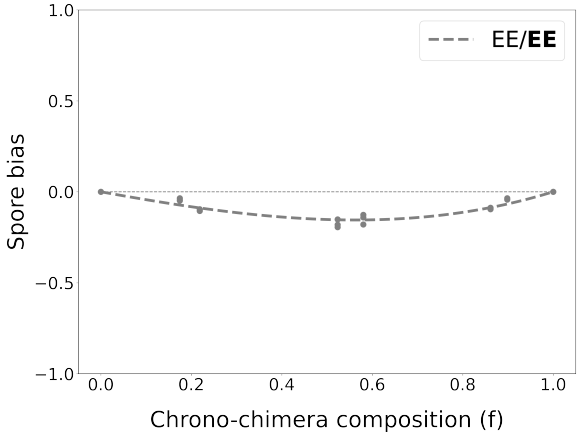

Figure S2: **AX3-GFP spore bias at the end of chimeric development with AX3-RFP cells.** The two populations were grown in co-cultures prior to aggregation to ensure they are in the same growth phase at the onset of the social cycle. Transformation with different plasmids introduced a spore bias (consistent when the transformation was repeated). We used this frequency-dependent bias to correct the measures realized in isogenic chronochimeras (main text and Methods).

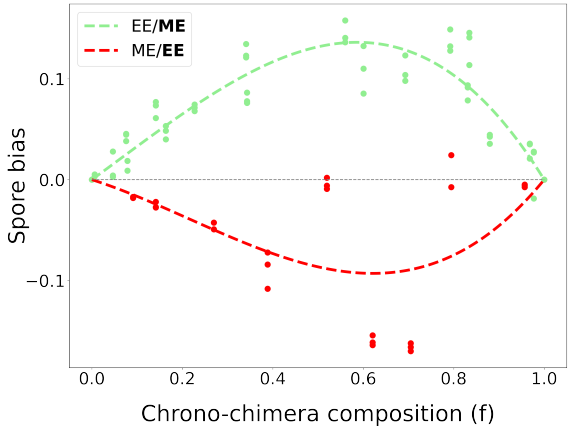

Figure S3: **Check for consistency of spore bias measures.** Corrected spore bias measured in two types of 'chrono-chimeras', using the AX3-GFP as the reference population: the AX3-GFP population was harvested in ME phase and mixed with a EE AX3-RFP population (light green line), and vice-versa (red line). Spore biases are reversed when the fluorescent labels are swapped, validating the use of the frequency correction.

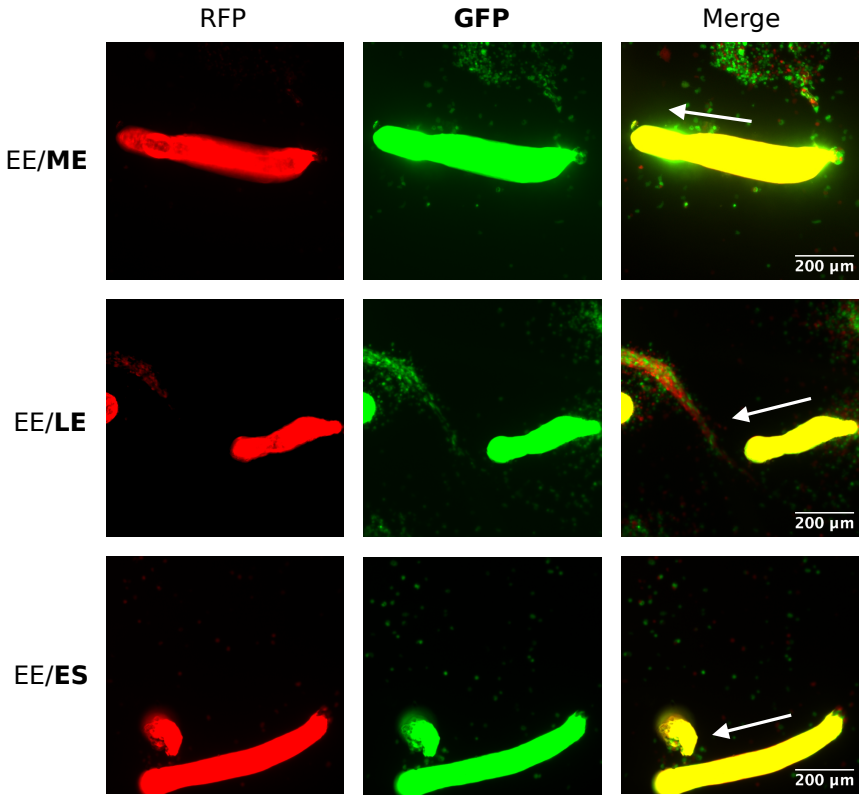

Figure S4: **Heterogeneity in populations growth phase at the onset of starvation does not translate into detectable cell sorting between the pre-spore and the pre-stalk regions of the slugs.** AX3-RFP cells harvested in EE phase of the growth cycle (first column) mixed in chimeras with AX3-GFP cells (second column) harvested either in ME (first row), LE (second row) or ES phase (third row) are uniformly spread along the slug axis (third colum). The white arrow indicates the direction of slug migration.

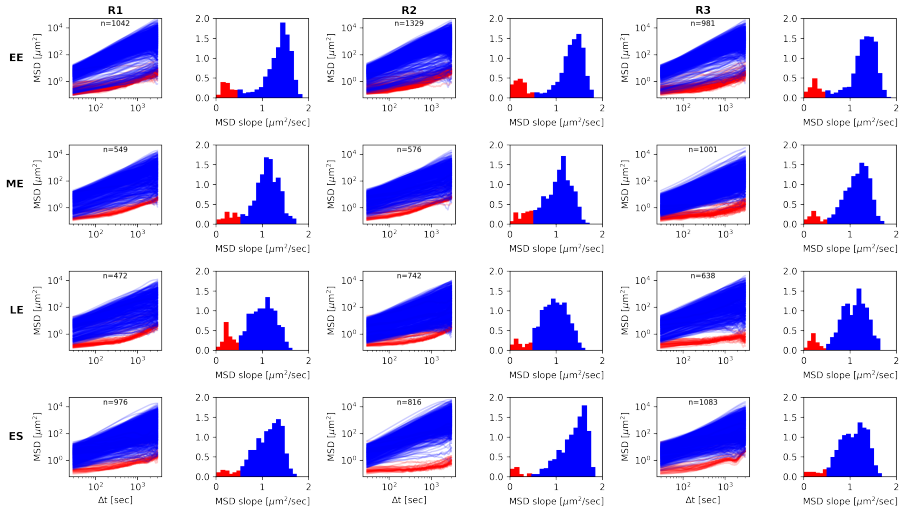

Figure S5: **Bimodal distribution of single cell motility depends on growth phase.** Individual mean square displacement of cells from populations harvested in EE, ME , LE and ES phase as a function of time lag (Δt). Cells were clustered into two classes based on the initial rate of increase of the MSD (slope of the log MSD vs log Δt, $\Delta t < 150$ secs, below or above the threshold value 0.5). As shown in Fig. 4 C, the proportion of cells belonging to the non-migrating class decreases in the course of vegetative growth.

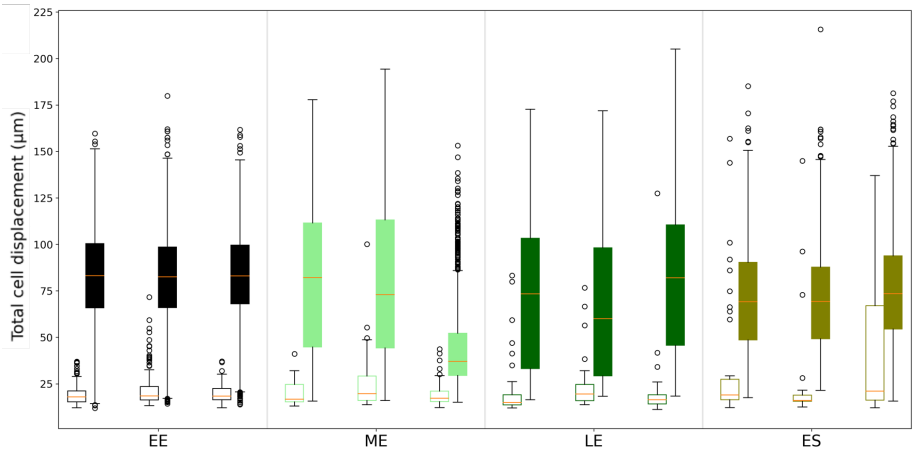

Figure S6: **Total cell displacement of cells harvested from populations in EE, ME, LE and ES phases.** Cells total displacement during the time of the experiment (1h) measured for the non-migrating cells class (empty boxes) and the migrating cells class (filled boxes) for populations harvested in EE, ME, LE and ES phase. Total displacement of non-migrating cells is significantly lower than that of migrating cells in every populations (Mann–Whitney U test, p-values < 0.0005). No significant variation in total displacement of migrating cells was observed between populations harvested in different growth phases (mixed effects model ANOVA, p-value=0.4691).

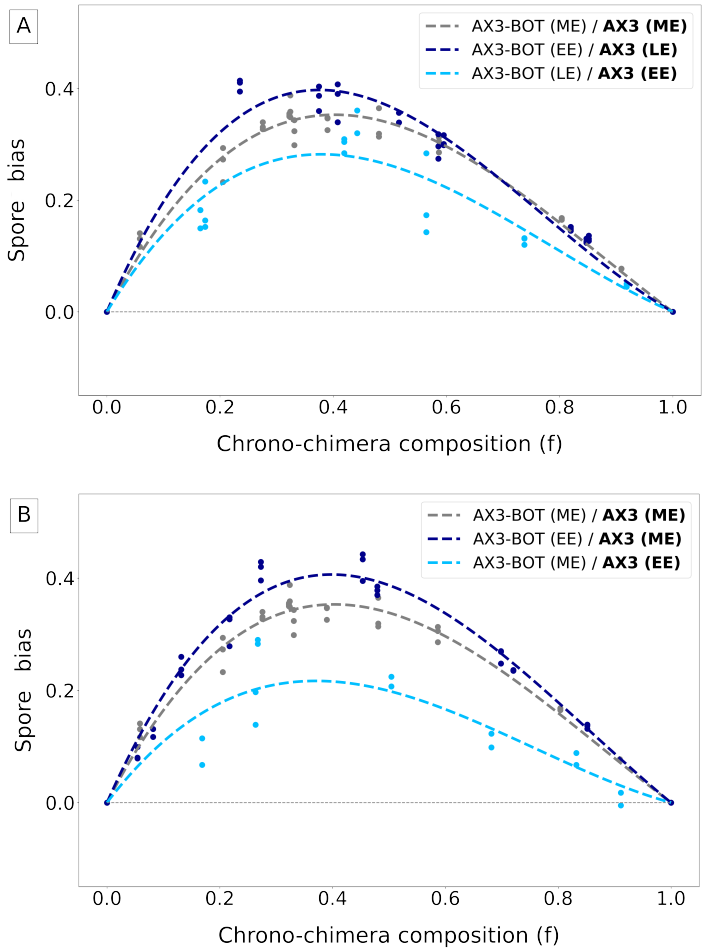

Figure S7: **Spore bias measured in chrono-chimeras with a lineage selected for increased adhesion**. Aggregation was initiated by mixing a strain that was obtained through experimental evolution for higher adhesiveness to the substratum (AX3-Bottom) with its ancestor (AX3). Three different combinations of growth phases are considered (as indicated in the legend). **A:** Strains are grown in co-culture and harvested in ME phase, the focal population is harvested in EE phase and the other in ME phase (dark blue line), or vice-versa (light blue line). **B:** Strains are grown in co-culture and harvested in ME phase, the focal population is harvested in EE phase and the other in LE phase (dark blue line), or vice-versa (light blue line). Spore bias variations are consistent whether the more advanced population is harvested in middle or late exponential phase, as it was observed for isogenic strains (Fig. 1), but starting from a high baseline bias.

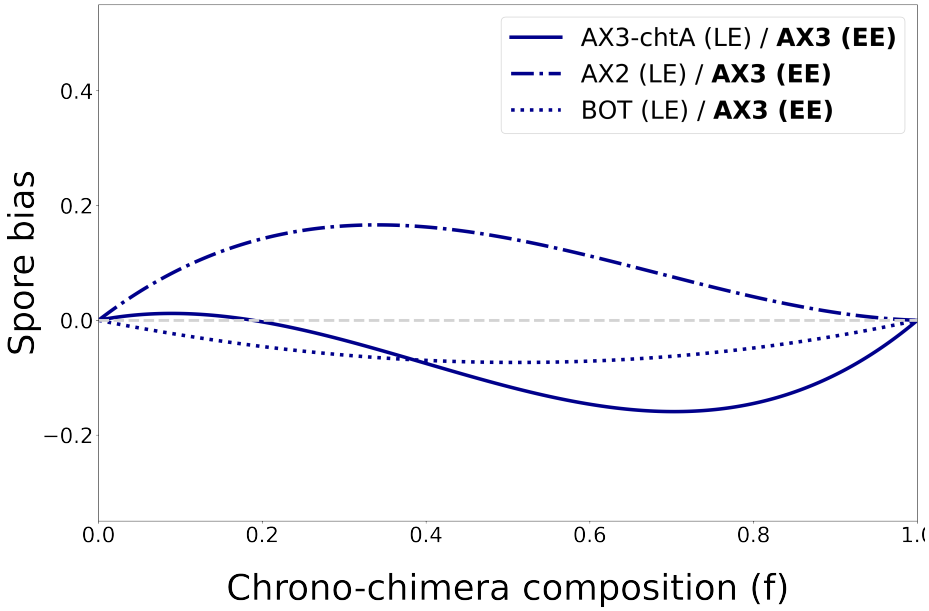

Figure S8: **Growth phase heterogeneity contribution to spore bias depends on genetic background**. Comparison of spore bias when the focal population AX3 (EE) is mixed with different strains in late exponential phase (LE). For every chimera, the curve indicates the deviation of the fitted spore bias from that for reference chimeras, where the two strains were harvested in the same growth phase (ME). The qualitative effect of growth differences is not consistent across the different chrono-chimeras, suggesting that it does not simply add up to variation induced by genetic differences, but depends instead on the genetic background.

References

Adiba, S., Forget, M., De Monte, S., 2022. Evolving social behaviour through selection of single-cell adhesion in Dictyostelium discoideum. iScience , 105006doi:10.1016/j.isci.2022.105006.

Allan, D.B., Caswell, T., Keim, N.C., van der Wel, C.M., 2018. trackpy: Trackpy v0.4.1. doi:10.5281/ZENODO.1226458.

Arias Del Angel, J.A., Nanjundiah, V., Benítez, M., Newman, S.A., 2020. Interplay of mesoscale physics and agent-like behaviors in the parallel evolution of aggregative multicellularity. EvoDevo 11, 21. doi:10.1186/s13227-020-00165-8.

Azhar, M., Kennady, P.K., Pande, G., Espiritu, M., Holloman, W., Brazill, D., Gomer, R.H., Nanjundiah, V., 2001. Cell cycle phase, cellular Ca2+ and development in Dictyostelium discoideum. The International Journal of Developmental Biology 45, 405–414.

Buttery, N.J., Rozen, D.E., Wolf, J.B., Thompson, C.R., 2009. Quantification of Social Behavior in D. discoideum Reveals Complex Fixed and Facultative Strategies. Current Biology 19, 1373–1377. doi:10.1016/j.cub.2009.06.058.

Buttery, N.J., Thompson, C.R.L., Wolf, J.B., 2010. Complex genotype interactions influence social fitness during the developmental phase of the social amoeba Dictyostelium discoideum. Journal of Evolutionary Biology 23, 1664–1671. doi:10.1111/j.1420-9101.2010.02032.x.

Coates, J.C., Harwood, a.J., 2001. Cell-cell adhesion and signal transduction during Dictyostelium development. Journal of Cell Science 114, 4349–4358. doi:10.1078/1434-4610-00039.

Dubravcic, D., van Baalen, M., Nizak, C., 2014. An evolutionarily significant unicellular strategy in response to starvation stress in Dictyostelium social amoebae. F1000Research 3. doi:10.12688/f1000research.4218.1.

Ennis, H.L., Dao, D.N., Pukatzki, S.U., Kessin, R.H., 2000. Dictyostelium amoebae lacking an F-box protein form spores rather than stalk in chimeras with wild type. Proceedings of the National Academy of Sciences 97, 3292–3297. doi:10.1073/pnas.97.7.3292.

Escalante, R., Wessels, D., Soll, D.R., Loomis, W.F., 1997. Chemotaxis to cAMP and slug migration in Dictyostelium both depend on migA, a BTB protein. Molecular Biology of the Cell 8, 1763–1775. doi:10.1091/mbc.8.9.1763.

Forget, M., Adiba, S., Brunnet, L.G., De Monte, S., 2022. Heterogeneous individual motility biases group composition in a model of aggregating cells. In revision .

Forget, M., Adiba, S., De Monte, S., 2021. Social conflicts in Dictyostelium discoideum : a matter of scales. Peer Community Journal 1, e58. doi:10.24072/pcjournal.39.

Fortunato, A., Queller, D.C., Strassmann, J.E., 2003a. A linear dominance hierarchy among clones in chimeras of the social amoeba Dictyostelium discoideum. Journal of Evolutionary Biology 16, 438–445. doi:10.1046/j.1420-9101.2003.00545.x.

Fortunato, A., Strassmann, J.E., Santorelli, L., Queller, D.C., 2003b. Co-occurrence in nature of different clones of the social amoeba, Dictyostelium discoideum. Molecular Ecology 12, 1031–1038. doi:10.1046/j.1365-294X.2003.01792.x.

Foster, K.R., Fortunato, A., Strassmann, J.E., Queller, D.C., 2002. The costs and benefits of being a chimera. Proceedings of the Royal Society of London. Series B: Biological Sciences 269, 2357–2362. doi:10.1098/rspb.2002.2163.

Garcia, T., Brunnet, L.G., De Monte, S., 2014. Differential adhesion between moving particles as a mechanism for the evolution of social groups. PLoS computational biology 10, e1003482. doi:10.1371/journal.pcbi.1003482.

Garcia, T., Doulcier, G., De Monte, S., 2015. The evolution of adhesiveness as a social adaptation. eLife 4, e08595. doi:10.7554/eLife.08595.

Gerisch, G., 1968. Chapter 6 Cell Aggregation and Differentiation in Dictyostelium, in: Current Topics in Developmental Biology. Elsevier. volume 3, pp. 157–197. doi:10.1016/S0070-2153(08)60354-3.

Gilbert, O.M., Foster, K.R., Mehdiabadi, N.J., Strassmann, J.E., Queller, D.C., 2007. High relatedness maintains multicellular cooperation in a social amoeba by controlling cheater mutants. Proceedings of the National Academy of Sciences 104, 8913–8917. doi:10.1073/pnas.0702723104.

Gomer, R.H., Jang, W., Brazill, D., 2011. Cell density sensing and size determination. Development, Growth & Differentiation 53, 482–494. doi:https://doi.org/10.1111/j.1440-169X.2010.01248.x, arXiv:https://onlinelibrary.wiley.com/doi/pdf/10.1111/j.1440-169X.2010.01248.x.

González-Velasco, De Las Rivas, Lacal, 2019. Proteomic and Transcriptomic Profiling Identifies Early Developmentally Regulated Proteins in Dictyostelium Discoideum. Cells 8, 1187. doi:10.3390/cells8101187.

Goury-Sistla, P., Nanjundiah, V., Pande, G., 2012. Bimodal distribution of motility and cell fate in Dictyostelium discoideum. International Journal of Developmental Biology 56, 263–272. doi:10.1387/ijdb.113384ps.

Gruenheit, N., Parkinson, K., Brimson, C.A., Kuwana, S., Johnson, E.J., Nagayama, K., Llewellyn, J., Salvidge, W.M., Stewart, B., Keller, T., van Zon, W., Cotter, S.L., Thompson, C.R.L., 2018. Cell cycle heterogeneity can generate robust cell type proportioning. Developmental Cell 47, 494–508.e4. doi:10.1016/j.devcel.2018.09.023.

Hiraoka, H., Nakano, T., Kuwana, S., Fukuzawa, M., Hirano, Y., Ueda, M., Haraguchi, T., Hiraoka, Y., 2020. Intracellular ATP levels influence cell fates in Dictyostelium discoideum differentiation. Genes to Cells 25, 312–326. doi:10.1111/gtc.12763.

Hirose, S., Benabentos, R., Ho, H.I., Kuspa, A., Shaulsky, G., 2011. Self-Recognition in Social Amoebae Is Mediated by Allelic Pairs of Tiger Genes. Science 333, 467–470. doi:10.1126/science.1203903.

Hofbauer, J., Sigmund, K., 1998. Evolutionary Games and Population Dynamics. 1 ed., Cambridge University Press. doi:10.1017/CBO9781139173179.

Houle, J., Balthazar, J., West, C.M., 1989. A glycosylation mutation affects cell fate in chimeras of Dictyostelium discoideum. Proceedings of the National Academy of Sciences 86, 3679–3683. doi:10.1073/pnas.86.10.3679.

Huang, H.J., Takagawa, D., Weeks, G., Pears, C., 1997. Cells at the Center ofDictyosteliumAggregates Become Spores. Developmental Biology 192, 564–571. doi:10.1006/dbio.1997.8769.

Kessin, R.H., 2001. Dictyostelium: Evolution, Cell Biology, and the Development of Multicellularity. Cambridge University Press. Google-Books-ID: rm7wHyUYSiAC.

Kubohara, Y., Arai, A., Gokan, N., Hosaka, K., 2007. Pharmacological evidence that stalk cell differentiation involves increases in the intracellular Ca2+ and H+ concentrations in Dictyostelium discoideum: H+, Ca2+ and cell differentiation. Development, Growth & Differentiation 49, 253–264. doi:10.1111/j.1440-169X.2007.00920.x.

Kuzdzal-Fick, J.J., Fox, S.A., Strassmann, J.E., Queller, D.C., 2011. High relatedness is necessary and sufficient to maintain multicellularity in Dictyostelium. Science (New York, N.Y.) 334, 1548–51. doi:10.1126/science.1213272.

Kuzdzal-Fick, J.J., Queller, D.C., Strassmann, J.E., 2010. An invitation to die: initiators of sociality in a social amoeba become selfish spores. Biology Letters 6, 800–802. doi:10.1098/rsbl.2010.0257.

Leach, C.K., Ashworth, J.M., Garrod, D.R., 1973. Cell sorting out during the differentiation of mixtures of metabolically distinct populations of *Dic-*

tyostelium discoideum. Development 29, 647–661. doi:10.1242/dev.29.3.647.

Loomis, W., 1971. Sensitivity of Dictyostelium discoideum to nucleic acid analogues. Experimental Cell Research 64, 484–486. doi:10.1016/0014-4827(71)90107-8.

Madgwick, P.G., Stewart, B., Belcher, L.J., Thompson, C.R.L., Wolf, J.B., 2018. Strategic investment explains patterns of cooperation and cheating in a microbe. Proceedings of the National Academy of Sciences 115, E4823–E4832. doi:10.1073/pnas.1716087115.

Maeda, Y., 2011. Cell-cycle checkpoint for transition from cell division to differentiation. Development, Growth & Differentiation 53, 463–481. doi:10.1111/j.1440-169X.2011.01264.x.

Martínez-García, R., Tarnita, C.E., 2016. Lack of ecological and life history context can create the illusion of social interactions in dictyostelium discoideum. PLOS Computational Biology 12, e1005246. doi:10.1371/journal.pcbi.1005246.

Mathavarajah, S., VanIderstine, C., Dellaire, G., Huber, R.J., 2021. Cancer and the breakdown of multicellularity: What idictyostelium discoideum/i , a social amoeba, can teach us. BioEssays 43, 2000156. doi:10.1002/bies.202000156.

McDonald, S.A., Durston, A.J., 1984. The cell cycle and sorting behaviour in Dictyostelium discoideum. Journal of Cell Science 66, 195–204.

Nagasaki, A., de Hostos, E.L., Uyeda, T.Q.P., 2002. Genetic and morphological evidence for two parallel pathways of cell-cycle-coupled cytokinesis in *Dictyostelium*. Journal of Cell Science 115, 2241–2251. doi:10.1242/jcs.115.10.2241.

Nanjundiah, V., 2019. Many roads lead to Rome: Neutral phenotypes in microorganisms. Journal of Experimental Zoology Part B: Molecular and Developmental Evolution 332, 339–348. doi:10.1002/jez.b.22909.

Parkinson, K., Buttery, N.J., Wolf, J.B., Thompson, C.R.L., 2011. A simple mechanism for complex social behavior. PLoS Biology 9, e1001039. doi:10.1371/journal.pbio.1001039.

Plak, K., Keizer-Gunnink, I., van Haastert, P.J.M., Kortholt, A., 2014. Rap1-dependent pathways coordinate cytokinesis in *Dictyostelium*. Molecular Biology of the Cell 25, 4195–4204. doi:10.1091/mbc.e14-08-1285.

Raper, K.B., 1940. Pseudoplasmodium formation and organization in Dictyostelium discoideum. Journal of the Elisha Mitchell Scientific Society 56.2, 241–282.

Rossine, F.W., Martinez-Garcia, R., Sgro, A.E., Gregor, T., Tarnita, C.E., 2020. Eco-evolutionary significance of "loners". PLOS Biology 18, e3000642. doi:10.1371/journal.pbio.3000642.

Sathe, S., Khetan, N., Nanjundiah, V., 2013. Interspecies and intraspecies interactions in social amoebae. Journal of Evolutionary Biology 27, 349–362. doi:10.1111/jeb.12298.

Sathe, S., Nanjundiah, V., 2018. Complex interactions underpin social behaviour in Dictyostelium giganteum. Behavioral Ecology and Sociobiology 72, 167. doi:10.1007/s00265-018-2572-9.

Schindelin, J., Arganda-Carreras, I., Frise, E., Kaynig, V., Longair, M., Pietzsch, T., Preibisch, S., Rueden, C., Saalfeld, S., Schmid, B., Tinevez, J.Y., White, D.J., Hartenstein, V., Eliceiri, K., Tomancak, P., Cardona, A., 2012. Fiji: an open-source platform for biological-image analysis. Nature Methods 9, 676–682. doi:10.1038/nmeth.2019.

Smith, J., Queller, D.C., Strassmann, J.E., 2014. Fruiting bodies of the social amoeba Dictyostelium discoideum increase spore transport by Drosophila. BMC evolutionary biology 14, 105. doi:10.1186/1471-2148-14-105.

Soll, D., Yarger, J., Mirick, M., 1976. Stationary phase and the cell cycle of Dictyostelium discoideum in liquid nutrient medium. Journal of Cell Science 20, 513–523. doi:10.1242/jcs.20.3.513.

Strassmann, J.E., Queller, D.C., 2011. Evolution of cooperation and control of cheating in a social microbe. Proceedings of the National Academy of Sciences 108, 10855–10862. doi:10.1073/pnas.1102451108.

Strassmann, J.E., Zhu, Y., Queller, D.C., 2000. Altruism and social cheating in the social amoeba Dictyostelium discoideum. Nature 408, 965–967. doi:10.1038/35050087.

Sucgang, R., Kuo, A., Tian, X., Salerno, W., Parikh, A., Feasley, C.L., Dalin, E., Tu, H., Huang, E., Barry, K., Lindquist, E., Shapiro, H., Bruce, D., Schmutz, J., Salamov, A., Fey, P., Gaudet, P., Anjard, C., Babu, M.M., Basu, S., Bushmanova, Y., van der Wel, H., Katoh-Kurasawa, M., Dinh, C., Coutinho, P.M., Saito, T., Elias, M., Schaap, P., Kay, R.R., Henrissat, B., Eichinger, L., Rivero, F., Putnam, N.H., West, C.M., Loomis, W.F., Chisholm, R.L., Shaulsky, G., Strassmann, J.E., Queller, D.C., Kuspa, A., Grigoriev, I.V., 2011. Comparative genomics of the social amoebae Dictyostelium discoideum and Dictyostelium purpureum. Genome Biology 12, R20. doi:10.1186/gb-2011-12-2-r20.

Tarnita, C.E., Washburne, A., Martinez-Garcia, R., Sgro, A.E., Levin, S.A., 2015. Fitness tradeoffs between spores and nonaggregating cells can explain the coexistence of diverse genotypes in cellular slime molds. Proceedings of the National Academy of Sciences 112, 2776–2781. doi:10.1073/pnas.1424242112.

Virtanen, P., Gommers, R., Oliphant, T.E., Haberland, M., Reddy, T., Cournapeau, D., Burovski, E., Peterson, P., Weckesser, W., Bright, J., van der Walt, S.J., Brett, M., Wilson, J., Millman, K.J., Mayorov, N., Nelson, A.R.J., Jones, E., Kern, R., Larson, E., Carey, C.J., Polat, , Feng, Y., Moore, E.W.,

VanderPlas, J., Laxalde, D., Perktold, J., Cimrman, R., Henriksen, I., Quintero, E.A., Harris, C.R., Archibald, A.M., Ribeiro, A.H., Pedregosa, F., van Mulbregt, P., SciPy 1.0 Contributors, Vijaykumar, A., Bardelli, A.P., Rothberg, A., Hilboll, A., Kloeckner, A., Scopatz, A., Lee, A., Rokem, A., Woods, C.N., Fulton, C., Masson, C., Häggström, C., Fitzgerald, C., Nicholson, D.A., Hagen, D.R., Pasechnik, D.V., Olivetti, E., Martin, E., Wieser, E., Silva, F., Lenders, F., Wilhelm, F., Young, G., Price, G.A., Ingold, G.L., Allen, G.E., Lee, G.R., Audren, H., Probst, I., Dietrich, J.P., Silterra, J., Webber, J.T., Slavič, J., Nothman, J., Buchner, J., Kulick, J., Schönberger, J.L., de Miranda Cardoso, J.V., Reimer, J., Harrington, J., Rodríguez, J.L.C., Nunez-Iglesias, J., Kuczynski, J., Tritz, K., Thoma, M., Newville, M., Kümmerer, M., Bolingbroke, M., Tartre, M., Pak, M., Smith, N.J., Nowaczyk, N., Shebanov, N., Pavlyk, O., Brodtkorb, P.A., Lee, P., McGibbon, R.T., Feldbauer, R., Lewis, S., Tygier, S., Sievert, S., Vigna, S., Peterson, S., More, S., Pudlik, T., Oshima, T., Pingel, T.J., Robitaille, T.P., Spura, T., Jones, T.R., Cera, T., Leslie, T., Zito, T., Krauss, T., Upadhyay, U., Halchenko, Y.O., Vázquez-Baeza, Y., 2020. SciPy 1.0: fundamental algorithms for scientific computing in Python. Nature Methods 17, 261–272. doi:10.1038/s41592-019-0686-2.

Yuen, I.S., Jain, R., Bishop, J.D., Lindsey, D.F., Deery, W.J., Van Haastert, P.J., Gomer, R.H., 1995. A density-sensing factor regulates signal transduction in Dictyostelium. Journal of Cell Biology 129, 1251–1262. doi:10.1083/jcb.129.5.1251, arXiv:https://rupress.org/jcb/article-pdf/129/5/1251/1264393/1251.pdf.

Zada-Hames, I.M., Ashworth, J.M., 1978. The cell cycle and its relationship to development in Dictyostelium discoideum. Developmental Biology 63, 307–320. doi:10.1016/0012-1606(78)90136-7.